Journal of Science and Technology in Civil Engineering, HUCE, 2025, 19 (4): 1–17

OPTIMIZATION STRATEGY OF MODEL B4TW-SCC IN PREDICTING SHRINKAGE OF SELF-COMPACTING CONCRETE

Nguyen Doan Binh[a,*], Wen-Cheng Liao[b]

[a]*Faculty of Building Materials, Hanoi University of Civil Engineering, No. 55 Giai Phong road, Bach Mai ward, Hanoi, Vietnam*
[b]*Department of Civil Engineering, College of Engineering, National Taiwan University, Taipei, Taiwan*

Article history:
Received 03/11/2025, Revised 18/12/2025, Accepted 22/12/2025

Abstract

Shrinkage strain directly reduces the dimensions of concrete, leading to potential intrusion of deleterious substances into the structure, affecting the durability in the long term, especially self-compacting concrete (SCC), which differs from conventional concrete in its composition, featuring a higher paste content and a lower amount of coarse aggregate, and consequential reduction in restraining capacity of aggregate. Most available models were designed to estimate the shrinkage strain of conventional concrete and lack the efficient prediction models of SCC. The enhancement in predicting could be applied to minimize the drawback of shrinkage on the building quality by preventing cracks and surface defects. Therefore, the new model B4TW-SCC was adjusted from the model B4, encompassing composition and compressive strength, to closely fit the newly collected database comprising 1316 test curves of shrinkage, assembled from numerous published papers. The paper presented a detailed optimal process based on both the minimum error of statistical indicators and the weighting scheme of the database to determine the important factors of the model B4TW-SCC for predicting the shrinkage of SCC. The evaluation results indicated that the developed model exhibited the highest efficiency with *NRMSE* values of only 52.3% and 50.5% in estimating autogenous shrinkage and total shrinkage among the current models for conventional concrete of B4, fib, and ACI, as well as the models for SCC, including CEB90-SCC (Poppe) and JSCE-SCC (Aslani).

Keywords: shrinkage; optimization; prediction; model; self-compacting concrete.

https://doi.org/10.31814/stce.huce2025-19(4)-01

1. Introduction

Deformation due to shrinkage occurs in an unloaded concrete structure when it is subjected to ambient conditions, such as temperature, humidity, and atmospheric air. Many types of shrinkage could be classified depending on the cause of moisture loss in concrete. When the shrinkage strain results in the internal tensile stress, cracks can be occurred rapidly in the element structure without external load, leading to a reduction in durability [1–3]. Shrinkage impacts can be excessive in mixtures of self-compacting concrete (SCC), which contains a higher paste content and a lower amount of coarse aggregate compared with conventional concrete [4–7]. Therefore, increasing shrinkage causes defacement of building surfaces and damage to the concrete due to environmental aggressiveness, such as water, carbon dioxide, and other organisms.

When analyzing the effects, not only the problem of safety against failure must be considered, but also important economic factors such as durability, serviceability, and long-term reliability relating to the cost for maintenance, repair, and inspection in the life cycle of construction [8]. Therefore, many available models have been designated to predict the shrinkage of plain concrete, such as ACI 209R-92 [9], CEB90 [10], fib MC2010 [11], AASHTO [12], GL2000 [13], JSCE [14], B3 [15, 16], B4

*Corresponding author. *E-mail address:* binhnd@huce.edu.vn (Binh, N. D.)

[17], and B4TW (Huang) [18]. Several presented models, including the model CEB90-SCC (Poppe) [19] and the model JSCE-SCC (Aslani) [20], were modified to estimate the shrinkage of SCC. These models still lack the accuracy to calculate the shrinkage due to the limitations of the testing data. The model CEB90-SCC was modified from CEB90 with only six designated mixtures, while the model JSCE-SCC was developed on 165 collected shrinkage data of SCC. Consequently, minor data results in biased models, which cannot evaluate exactly different cases of shrinkage.

The shrinkage behaviour is influenced by many complex factors, such as the content and properties of used materials, curing conditions, and environment, resulting in consequent difficulty in shrinkage prediction [21]. Besides, the calibration of the prediction model requires an adequate database. However, most of the available databases were assembled on the shrinkage research of conventional concrete [22–24]. Therefore, a fully adequate database is required to calibrate the formulae and parameters of the present model for predicting autogenous shrinkage strain and total shrinkage strain.

This study focused on developing an optimal process to establish a highly efficient set of parameters for the prediction model B4TW-SCC, which would yield acceptable statistical coefficients with minimal error and unbiased data based on the weighting scheme of the database. The new model was developed by modifying of the models B4 and B4TW (Huang) to closely fit the new database, which contains a total of 1,136 datasets on shrinkage. The calibration procedure was also introduced in clear steps, from autogenous shrinkage to total shrinkage of SCC, using pure cement or combining mineral admixtures. Moreover, the improved model demonstrated a better prediction capacity compared to other available models for shrinkage strain.

2. SCC database of shrinkage

The autogenous shrinkage and total shrinkage considered in the SCC database were compiled from research papers published since 1995. The SCC database comprised 215 curves of autogenous shrinkage based on unsealed specimens and 1101 curves of total shrinkage corresponding to sealed specimens. The range of the new laboratory database and the application scope of model B4TW-SCC are limited as listed in Table 1, including curing temperature (T_{cur}), compressive strength at age of 28 days (f_{cm28}), cementitious material (cm), water to cementitious material ratio (w/cm), aggregate to cementitious material ratio (a/cm), coarse aggregate (ca), volume to surface area ratio (V/S). Additionally, the mineral admixtures were limited to a range of 0–70 %/cm, except for silica fume (SF), which was limited to a range of 0–15 %/cm.

Table 1. Application range of model B4TW-SCC

Range	T_{cur} (ºC)	f_{cm28} (MPa)	cm (kg/m^3)	w/cm	a/cm	ca (kg/m^3)	V/S (mm)
Min	20.0	17	283	0.18	1.60	420	11.3
Max	30.0	110	840	0.64	6.74	1300	70.0
Median	22.0	57	500	0.35	3.31	838	21.4
Mean	21.7	52	506	0.36	3.40	842	20.9
Standard deviation	1.9	19	84	0.07	0.73	100	5.4

The distribution range of the main parameters is presented in Fig. 1. According to the distribution of the datasets, the 28-day compressive strength ranges from 17 to 110 MPa, covering both normal compressive strength ($f_{cm28} \leq 55$ MPa) and high compressive strength ($f_{cm28} > 55$ MPa). The average values of parameters include w/cm of 0.36, a/cm of about 3.4, cm of approximately 500 kg/m^3, and ca of 840 kg/m^3. These values would be applied to modify the equations in the model B4TW-SCC.

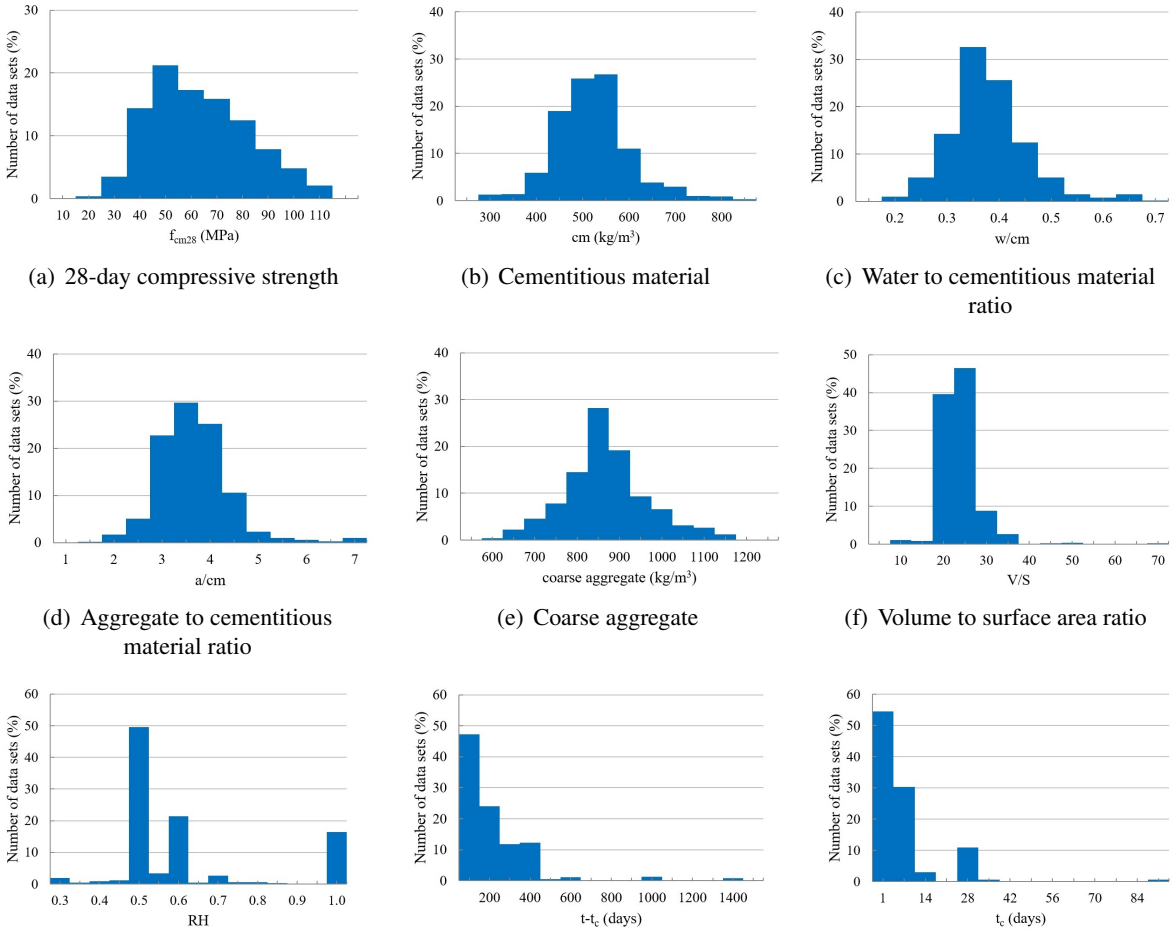

(a) 28-day compressive strength (b) Cementitious material (c) Water to cementitious material ratio

(d) Aggregate to cementitious material ratio (e) Coarse aggregate (f) Volume to surface area ratio

(g) Relative humidity (h) Test duration (i) Start of test

Figure 1. Distribution of the SCC database

According to the results presented in Fig. 2(a), different types of cement were classified based on their components and hydration capacity with water [17]. In which ordinary Portland cement (type R) was the majority proportion, with the datasets approaching approximately 78 % in total. Additionally, the last cement types achieved only 13 % of low-heat cement, classified as type SL, and 9 % of high-heat cement, designated as type RS. Therefore, the database of SCC containing pure cement was selected to calibrate the shrinkage equations of model B4TW-SCC, which determined the parameters in the optimization procedure.

Generally, the supplementary cementitious materials were incorporated in the mixture component of SCC. Fig. 2(b) shows clearly the types of powder used in the composition of SCC. In which the fillers, including limestone powder and crushed sand, had a rate of approximately 21 %, and mineral admixtures involving fly ash, slag, silica fume, and other pozzolanic materials, contain about 59 %. In contrast, the number of datasets using SCC with pure cement is 20 %. Additionally, limestone powder was a popular type of filler in SCC, while fly ash (FA) was considered the predominant type, comprising the highest proportion over 25 % among the mineral admixtures in SCC ingredients. Besides, the ground-granulated blast furnace slag (GGBS) and the combination of GGBS with FA have a range of about 7 % to 8 %. SF was used at the lowest proportion in SCC composition, and this

material was obtained in only 3 % of the samples. The other pozzolanic materials, such as rice husk ash and metakaolin, were used in over 15 % of the SCC database. In the database, the aggregate was classified into different types, including diabase, quartzite, limestone, granite, and sandstone, which had a nominal maximum size ranging from 9.5 mm to 25 mm and a mean value of approximately 16 mm.

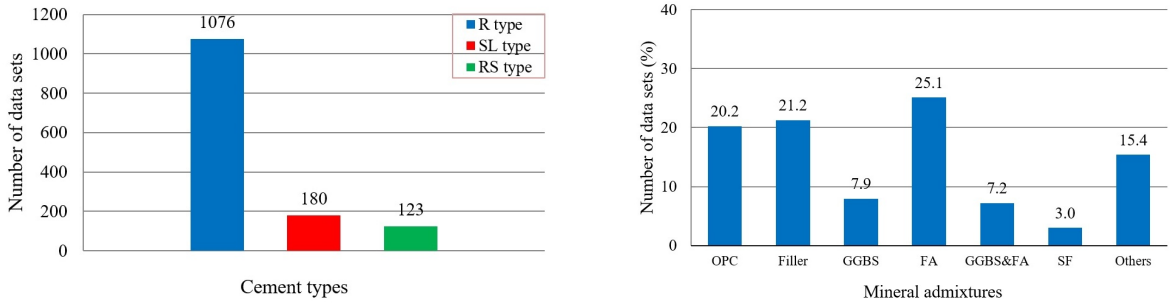

(a) Cement types (b) Mineral admixtures

Figure 2. Cement types and mineral admixtures of the SCC database

3. Prediction model B4TW-SCC for shrinkage of SCC

The model B4TW-SCC was improved on average composition values of the a/cm ratio, w/cm ratio, cm, and coarse aggregate were approximately 0.36, 3.4, 500 kg/m^3, and 840 kg/m^3 based on the SCC database, respectively. Moreover, a new set of parameters was optimized for autogenous and total shrinkage of SCC using ordinary Portland cement. The model B4TW-SCC also introduced novel scaling factors to modify the shrinkage prediction of SCC containing the fine powders and supplementary cementitious materials, which are used widely to enhance the concrete properties. This issue is another significant difference from the original model B4, which was designed to predict the time-dependent deformation of conventional concrete using mostly chemical additives. The determination process of all model parameters will be discussed in the next section of the optimization strategy.

The formulae of total shrinkage strain can be expressed as

$$\varepsilon_{cs}(\tilde{t},\tilde{t}_c) = \varepsilon_{sh}(\tilde{t},\tilde{t}_c) + \varepsilon_{au}(\tilde{t},\tilde{t}_c) - \varepsilon_{au}(\tilde{t}_c) \tag{1}$$

where $\varepsilon_{cs}(\tilde{t},\tilde{t}_c)$ is total shrinkage strain (10^{-6} m/m); $\tilde{t}$ is the temperature-adjusted test duration (days); $\tilde{t}_c$ is the temperature-adjusted start of test (days); $\varepsilon_{sh}(\tilde{t},\tilde{t}_c)$ is the drying shrinkage strain (10^{-6} m/m); $\varepsilon_{au}(\tilde{t},\tilde{t}_c)$ is autogenous shrinkage strain at $\tilde{t}$ days, and $\varepsilon_{au}(\tilde{t}_c)$ is the autogenous shrinkage strain at $\tilde{t}_c$ days (10^{-6} m/m).

$$\tilde{t} = (t - t_c)\beta_{Ts} \tag{2}$$

$$\beta_{Ts} = \exp\left[\frac{U_s}{R}\left(\frac{1}{293} - \frac{1}{T+273}\right)\right] \tag{3}$$

$$\tilde{t}_c = t_c\beta_{Th} \tag{4}$$

$$\beta_{Th} = \exp\left[\frac{U_h}{R}\left(\frac{1}{293} - \frac{1}{T_{cur}+273}\right)\right] \tag{5}$$

where T is the testing temperature (°C), T_{cur} is the curing temperature (°C), t is the age of concrete (days), t_c is the start of testing age (days), and $U_s/R, U_h/R$ could be taken 4000 K [22].

3.1. Autogenous shrinkage

The autogenous shrinkage equation of the model B4TW-SCC was presented as

$$\varepsilon_{au}(\tilde{t},\tilde{t}_c) = \varepsilon_{au\infty}\left[1+\left(\frac{\tau_{au}}{\tilde{t}+\tilde{t}_c}\right)^{\alpha}\right]^{r_t} \tag{6}$$

Final autogenous shrinkage can be expressed as

$$\varepsilon_{au\infty} = -f_{au,cem}\varepsilon_{au,cem}\left(\frac{a/cm}{3.4}\right)^{r_{\varepsilon a}}\left(\frac{w/cm}{0.36}\right)^{f_{au,wc}r_{\varepsilon w}} \tag{7}$$

Autogenous shrinkage halftime is expressed as follows

$$\tau_{au} = \tau_{au,cem}\left(\frac{w/cm}{0.36}\right)^{r_{\tau w}} \tag{8}$$

$$\alpha = r_{\alpha}\left(\frac{w/cm}{0.36}\right) \tag{9}$$

where $\varepsilon_{au\infty}$ is final autogenous shrinkage (10^{-6} m/m); τ_{au} is autogenous shrinkage halftime; $r_{\varepsilon w}$, $r_{\varepsilon a}$, $\varepsilon_{au,cem}$, $r_{\tau w}$, r_t, r_{α}, and $\tau_{au,cem}$ are the parameters of autogenous shrinkage, as given in Table 2; $f_{au,cem}$, $f_{au,wc}$ are the scaling factors of SCC containing mineral admixture for autogenous shrinkage, as presented in Table 4.

Table 2. Parameters for autogenous shrinkage of SCC using pure cement

Cement	$r_{\varepsilon w}$	$r_{\varepsilon a}$	$\varepsilon_{au,cem}$	$r_{\tau w}$	r_t	r_{α}	$\tau_{au,cem}$
Type R	−2.5	−0.65	$250\cdot10^{-6}$	3.5	−3.0	1	1

Table 3. Parameters for drying shrinkage of SCC using pure cement

Cement	$p_{\varepsilon w}$	$p_{\tau w}$	$p_{\varepsilon a}$	$p_{\tau a}$	$p_{\varepsilon c}$	$p_{\tau c}$	$p_{\varepsilon ca}$	ε_{cem}	τ_{cem} (day)
Type R	1.10	−0.04	−0.6	−0.30	0.07	−0.05	0.35	$440\cdot10^{-6}$	0.016

Table 4. Scaling factors of SCC containing admixtures

Admixture type (% of *cm*)	Scaling factors			
	$f_{au,cem}$	$f_{au,wc}$	$f_{sh,cem}$	$f_{sh,\tau}$
Filler	1.2	0.6	1.0	1.0
Slag	1.3	0.8	0.85	1.0
Fly ash	1.05	0.9	1.15	0.95
Slag and fly ash	1.0	0.7	1.1	1.0
Silica fume	1.0	0.75	1.0	1.0
Slag and silica fume	1.5	1.0	0.9	1.1
Fly ash and silica fume	0.95	0.5	1.15	0.85
Slag, fly ash, and silica fume	0.95	0.6	0.85	1.15
Last admixtures	0.95	0.7	0.9	1.0

3.2. Drying shrinkage

The shrinkage strain in drying conditions is followed as

$$\varepsilon_{sh}\left(\tilde{t},\tilde{t}_c\right)=f_{sh,cem}\varepsilon_{shu}\left(\tilde{t}_c\right)k_hS\left(\tilde{t}\right) \tag{10}$$

The time curve is expressed as

$$S\left(\tilde{t}\right)=\tanh\sqrt{\frac{\tilde{t}}{f_{sh,\tau}\tau_{sh}}} \tag{11}$$

Humidity dependence is expressed as

$$k_h=\begin{cases}1-RH^3 & \text{for } RH\le 0.98\\ 12.94\left(1-RH\right)-0.2 & \text{for } 0.98\le RH\le 1\end{cases} \tag{12}$$

The ultimate drying shrinkage is calculated as

$$\varepsilon_{shu}\left(\tilde{t}_c\right)=-\varepsilon_0k_{\varepsilon\alpha}\frac{E\left(7\beta_{Th}+600\beta_{Ts}\right)}{E\left(\tilde{t}_c+\tau_{sh}\beta_{Ts}\right)} \tag{13}$$

The modulus of elasticity can be predicted as follows

$$E_{cmt}=4734\sqrt{f_{cmt}} \tag{14}$$

$$f_{cmt}=\left(\frac{t}{4+0.85\cdot t}\right)f_{cm28} \tag{15}$$

$$\varepsilon_0=\varepsilon_{cem}\left(\frac{a/cm}{3.4}\right)^{p_{\varepsilon a}}\left(\frac{w/cm}{0.36}\right)^{p_{\varepsilon w}}\left(\frac{4.6cm}{\rho}\right)^{p_{\varepsilon c}}\left(\frac{ca}{840}\right)^{p_{\varepsilon ca}} \tag{16}$$

$$\tau_{sh}=\tau_0k_{\tau a}(k_sD)^2 \tag{17}$$

$$\tau_0=\tau_{cem}\left(\frac{a/cm}{3.4}\right)^{p_{\tau a}}\left(\frac{w/cm}{0.36}\right)^{p_{\tau w}}\left(\frac{4.6cm}{\rho}\right)^{p_{\tau c}} \tag{18}$$

The specimen size is expressed as

$$D=2V/S \tag{19}$$

The factors depending on aggregate types $k_{\tau a}$ and $k_{\varepsilon a}$ are given as follows [17, 18]

$$k_{\tau a}=\begin{cases}0.06 & \text{for diabase}\\ 0.59 & \text{for quartzite}\\ 1.80 & \text{for limestone}\\ 4.00 & \text{for granite}\\ 2.70 & \text{for sandstone}\end{cases} \tag{20}$$

$$k_{\varepsilon a}=\begin{cases}0.76 & \text{for diabase}\\ 0.71 & \text{for quartzite}\\ 0.95 & \text{for limestone}\\ 1.05 & \text{for granite}\\ 2.00 & \text{for sandstone}\end{cases} \tag{21}$$

where ρ is the volume density of concrete (kg/m^3); RH is the relative humidity; E_{cmt} is t-day modulus of elasticity (MPa), f_{cmt} and f_{cm28} are compressive strength at t and 28 days, respectively; ε_0 is the final drying shrinkage; τ_{sh} is the halftime drying shrinkage; k_s is shape parameter as given in the model B4 [17]; $p_{\varepsilon w}$, $p_{\tau w}$, $p_{\varepsilon a}$, $p_{\tau a}$, $p_{\varepsilon c}$, $p_{\tau c}$, $p_{\varepsilon ca}$, ε_{cem}, and τ_{cem} are the parameters of drying shrinkage, as listed in Table 3; $f_{sh,cem}$, $f_{sh,\tau}$ are the scaling factors of SCC using mineral admixture for drying shrinkage, as summarized in Table 4.

3.3. Optimization strategy

The optimum parameters of the model B4TW-SCC, summarized in Tables 2–4, were determined using statistical indicators including the determination coefficient R^2 [25, 26] and NRMSE [27, 28]. Factor R^2 can rapidly indicate the compatibility of the formulae in the prediction model with the test data in the regression model. This coefficient can evaluate the model within an allowable range of 0 to 1, whereas NRMSE typically analyzes the error of the prediction model, with the result expressed as a percentage. However, if only minimum errors of the statistical coefficients were made, then a biased model would be obtained. This result is clearly evident in the distribution range of parameters in the shrinkage database of SCC, as shown in Fig. 1. Generally, the laboratory data tend to fall in large portions within short-term test durations, small sample dimensions, and early start times of testing. These datasets would impact the results of statistical coefficients, leading to a biased evaluation of the prediction model.

In this paper, the optimization strategy suggests combining statistical coefficients and a weighting plan to achieve an unbiased model in fitting the database [29, 30]. The evaluation of shrinkage prediction would be based on acceptable statistical coefficients with a proper number of subsets for independent variables, which belong to the extrinsic factors [31]. According to the SCC database, the independent variables of autogenous shrinkage and total shrinkage were divided into a typical range, as summarized in Tables 5 and 6, respectively.

Table 5. The subsets of autogenous shrinkage variables

$t - t_c$ (days)		t_c (days)	
Subset	Data volume	Subset	Data volume
≤ 90	120	< 1	119
90-210	54	≥ 1	96
210-1500	41		

Table 6. The subsets of total shrinkage variables

$t - t_c$ (days)		V/S (mm)		RH (%)		t_c (days)	
Subset	Data volume	Subset	Data volume	Subset	Data volume	Subset	Data volume
≤ 90	392	11.3-18	444	27-50	688	≤ 1	464
90-210	388	18-23	479	50-60	340	1-7	427
210-1500	321	23-70	178	60-90	73	7-90	210

The flow diagram of the model calibration process is illustrated in Fig. 3. There are two steps applied sequentially from autogenous shrinkage (step 1) to drying shrinkage (step 2) with different stages. In stage I, the optimization was first performed for SCC using only Portland cement, which was considered as basic formulation. The initial parameter values for autogenous shrinkage and

total shrinkage should be set to 7 and 9, respectively. Subsequent refinement was carried out on the scaling factors of SCC using mineral admixtures with nine cases in stage II. Therefore, the optimum parameters were 18 for each type of shrinkage.

The optimum procedure started sequentially from the most important parameters to the least ones. The calibration must be performed from autogenous shrinkage to total shrinkage, while the influential roles of the parameters were decided upon in order. The shrinkage parameters of sealed specimens were determined with the different subsets of the independent variables based on test duration and testing age of the collected database, without the impact of the humidity conditions. After that, the drying shrinkage of unsealed specimens was carried out to determine the parameters based on fixed formulae of autogenous shrinkage and the subsets of the total shrinkage variables in the drying conditions. The unsealed specimens are significantly influenced by ambient conditions; therefore, subsets of specimen size and environmental humidity were considered in the optimal process.

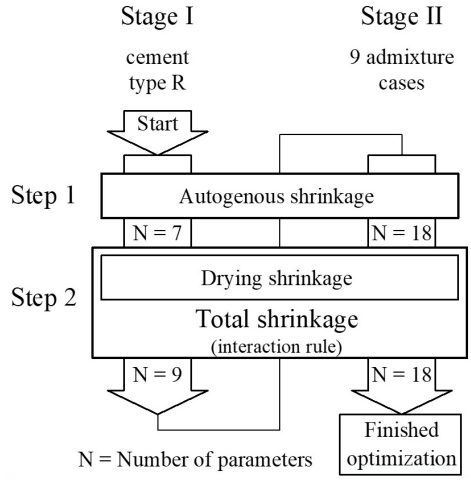

Figure 3. Optimization strategy of B4TW-SCC for shrinkage

3.4. Optimization parameters of SCC using pure cement

The optimization was carried out to determine the shrinkage parameters of SCC using only cement in the initial step. The shrinkage formulae were adjusted by the average composition of the SCC database with new values of $w/cm, a/cm, cm$, and coarse aggregate corresponding to 0.36, 3.4, 4.6, and 840, respectively. In which the parameter of cm was obtained from the division of the unit weight of concrete ($\rho = 2350$ kg/m^3 in the undetermined case) by the cement content. The process was carried out sequentially on influential role parameters to examine the shrinkage behaviour. The optimal results of the parameters were selected based on a combination of acceptable statistical values for the determination coefficient (R^2) and *NRMSE*, using subsets of the database and a visual assessment of the data distribution through a diagram. The diagram comprises the axes of test data (x-axis), predicted value (y-axis), a standard line ($x = y$), and an acceptable range of ±40 % with two red dashed lines.

a. Autogenous shrinkage

Two types of autogenous shrinkage variables, including test duration and testing age, were divided into subsets, as summarized in Table 5. In which large proportions of the autogenous shrinkage database had the test duration below 90 days, and the testing age was under 1 day. Based on the subsets of the database, the parameter $r_{\varepsilon w}$ was optimized with a value of −2.5, as shown in the results in Fig. 4. This value needs to satisfy the acceptable errors of the subsets in all independent variables, including test duration ($t - t_c$) and testing age (t_c). Similarly, the last parameters of autogenous shrinkage, including $r_{\varepsilon a}, \varepsilon_{au,cem}, r_{\tau w,rt}, r_\alpha$, and $\tau_{au,cem}$ were carried out, and the results were presented in Table 2. Consequently, the prediction capacity of the modified model B4TW-SCC based on the optimum parameter improved more significantly than that of the original model B4, as shown in Fig. 5. The data points of the model B4TW-SCC were distributed closely around the standard line

($x = y$). Additionally, the values of R^2 and *NRMSE* for this model, at 0.62 and 43.45 %, were better than those of the B4 model, with R^2 and *NRMSE* of 0.43 and 53.06 %, respectively.

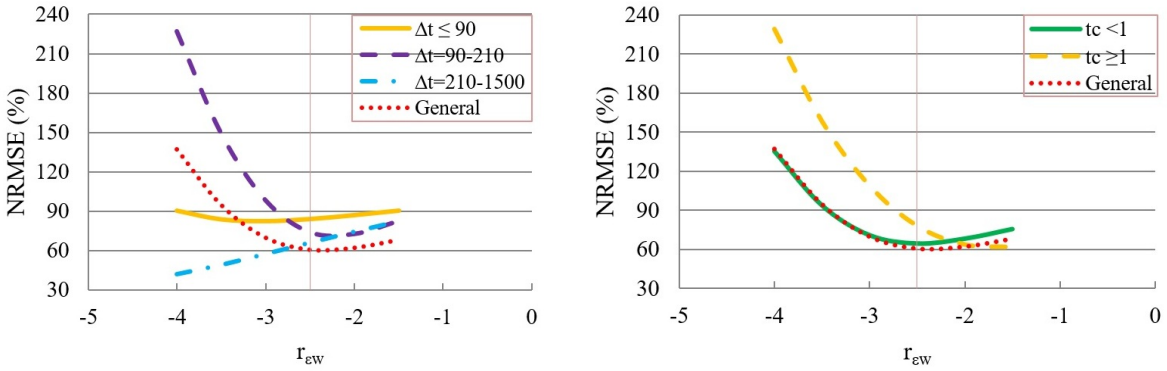

(a) $t - t_c$ (days) (b) t_c (days)

Figure 4. Optimum parameter $r_{\varepsilon w}$ of SCC with pure cement

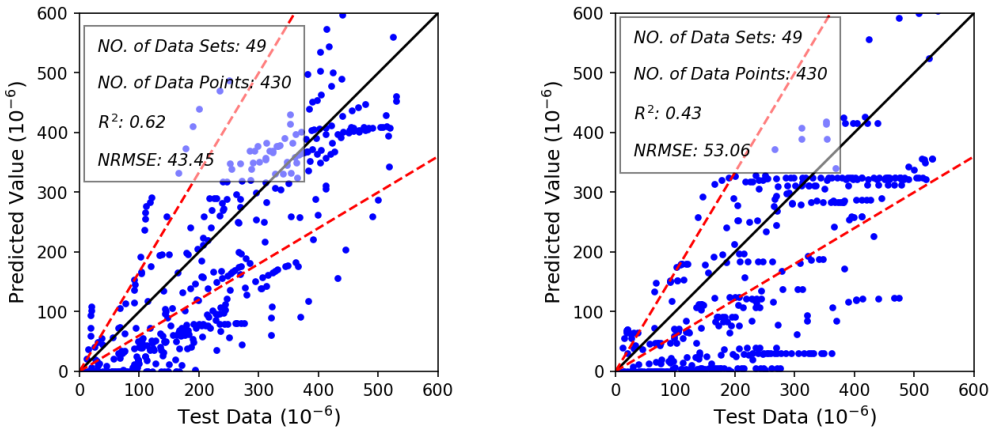

(a) Model B4TW-SCC (b) Model B4

Figure 5. Influence of optimum parameter on autogenous shrinkage prediction of SCC with pure cement

b. Total shrinkage

Total shrinkage was calculated as summary of autogenous shrinkage and drying shrinkagein the formulae of model B4TW-SCC. Therefore, the optimization of total shrinkage was carried out based on fixed parameters of autogenous shrinkage and calibrating the parameters of drying shrinkage. However, total shrinkage had to consider a greater number of independent variables than autogenous shrinkage, including test duration ($t-t_c$), specimen size (V/S), relative humidity (RH), and start of test (t_c). These variables were divided into subsets with proper data numbers, as summarized in Table 6.

Based on the subsets of the database, the parameter $p_{\varepsilon w}$ was optimized with values of 1.1, as illustrated in Fig. 6. Moreover, the other parameters of SCC without mineral admixtures were carried out similarly to the $p_{\varepsilon w}$. The optimum results of all parameters $p_{\varepsilon w}, p_{\tau w}, p_{\varepsilon a}, p_{\tau a}, p_{\varepsilon c}, p_{\tau c}, p_{\varepsilon ca}, \varepsilon_{cem}$, and τ_{cem} in predicting total shrinkage are listed in Table 3. The predicted values of the model B4TW-SCC were remarkably adequate for the test data, with an *NRMSE* of 50.6 %. In contrast, the model B4

significantly underestimated the total shrinkage of SCC, resulting in an error of 84.8 %, as shown in Fig. 7. This comparison clearly indicates that the improvement of the modified model is based on the optimum parameters. The number of parameters was calibrated to fit the SCC database, encompassing up to 16 values for total shrinkage, including seven parameters for autogenous shrinkage and nine parameters for drying shrinkage.

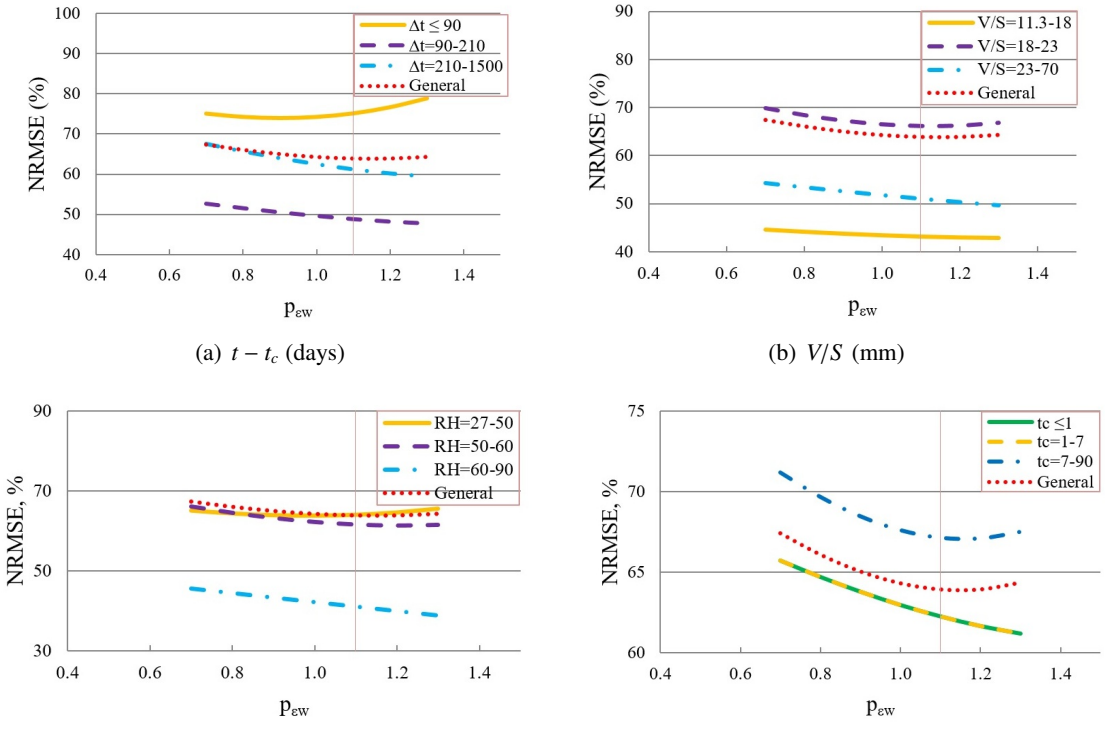

(a) $t - t_c$ (days) (b) V/S (mm)

(c) RH (d) t_c (days)

Figure 6. Optimum parameter $p_{\varepsilon w}$ for drying shrinkage of SCC using pure cement

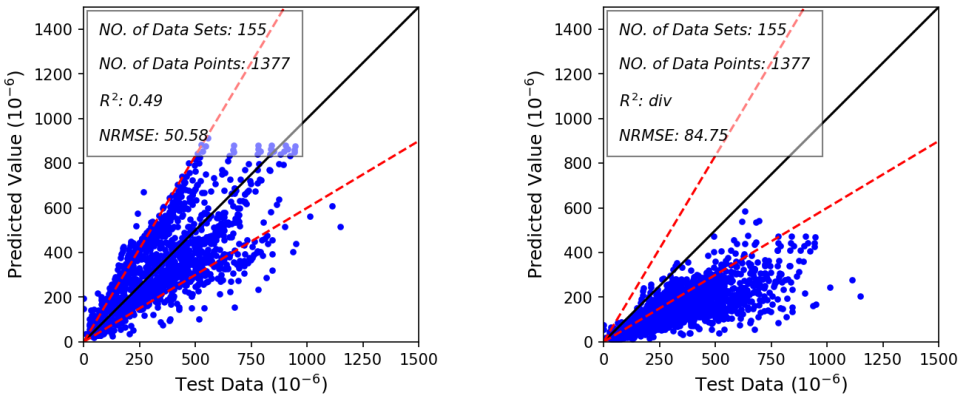

(a) B4TW-SCC model (b) B4 model

Figure 7. Influence of optimum parameter of SCC using pure cement for total shrinkage

3.5. Optimization parameters of SCC using mineral admixtures

The scaling parameters were used to adjust the shrinkage prediction of SCC using mineral admixtures and fine powders, as presented in the database. These materials are highly popular in the ingredient composition of SCC, enhancing its workability and mechanical properties compared to conventional concrete. Moreover, the mineral admixtures could also significantly influence the shrinkage behaviour in case these materials partially replace cement in SCC composition. For instance, the incorporation of fly ash could decrease significantly autogenous shrinkage over 20 %, which was studied by Chan et al. [32] and Kristiwan et al. [33]. Additionally, the total shrinkage was also enhanced by partially replacing of cement content with fly ash [34–36]. However, SCC combining slag increases the autogenous shrinkage higher than plain concrete [32, 37]. The negative influences of slag on total shrinkage have been reported by Güneyisi et al. [4], Zhao et al. [35], and Yasumoto et al. [38]. In contrast, other authors have indicated that total shrinkage increases with the rise of slag content [32, 37, 39]. Therefore, determining the factors was necessary to enhance the predictive capacity of the model for various types of cement replacement materials in the SCC.

The scaling factors of SCC using mineral admixture start at one as the original values. Then the optimization process is performed similarly to the parameters of concrete with pure cement, based on the independent variables. The results of scaling factors were determined on the minimum errors of statistical indicators and the visual assessment of the distribution between calculated values and test data. The new values of scaling factors also indicated the impact of mineral admixtures on the shrinkage behaviour of SCC through the reaction capacity with cement in the hydration process.

According to the results given in Fig. 8, the SCC using fly ash is presented to determine the scaling factors of autogenous shrinkage in the optimum procedure. It is clearly seen that the parameter $f_{au,wc}$ of autogenous shrinkage has an optimum value of 0.9 based on subsets of test duration and testing age. Additionally, the parameter $f_{sh,cem}$ of drying shrinkage was found to be 1.15 (Fig. 9), which is an acceptable result considering the independent variables, including test duration, specimen size, relative humidity, and start of test [31]. The last parameters of SCC using mineral admixtures were carried out similarly to $f_{au,wc}$, and $f_{sh,cem}$. As a result, all values of scaling parameters were summarized in Table 4. These parameters of the model B4TW-SCC were also the significant differences from those of the model B4, which was designed to predict the shrinkage of concrete using the chemical additives.

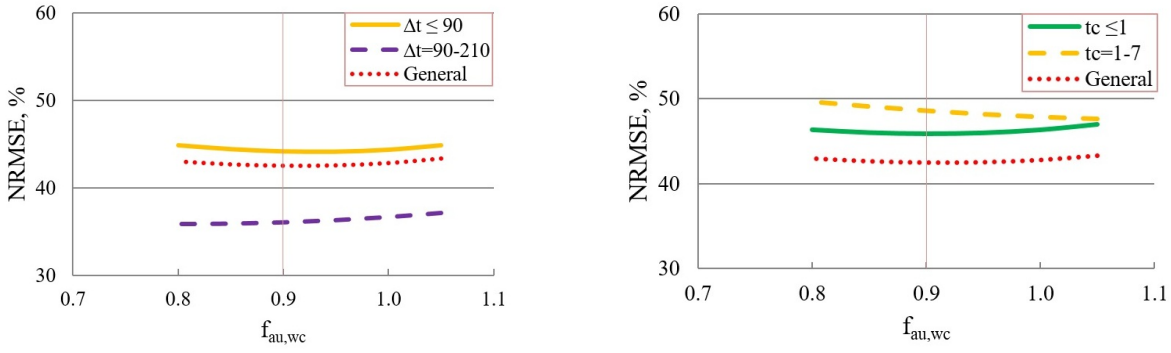

(a) $t - t_c$ (days) (b) t_c (days)

Figure 8. Optimum parameter $f_{au,wc}$ for autogenous shrinkage of SCC using FA

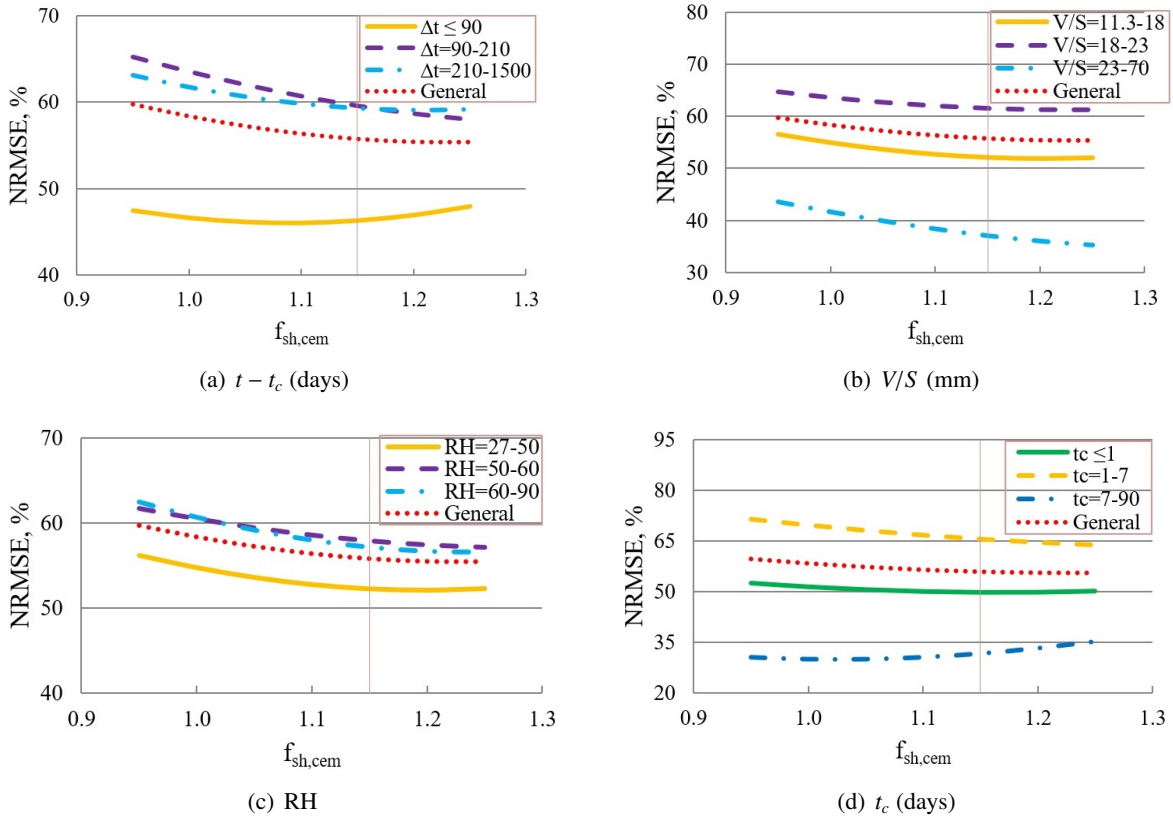

(a) $t - t_c$ (days) (b) V/S (mm)

(c) RH (d) t_c (days)

Figure 9. Optimum parameter $f_{sh,cem}$ for drying shrinkage of SCC using FA

4. Comparison of the prediction model B4TW-SCC with other models

Based on optimum values of parameters, the B4TW-SCC model was improved better than the original model and other available models, which have key formulae as presented in Table 7. The evaluation of the modified model is based on autogenous shrinkage of 165 datasets and total shrinkage of 843 datasets, as shown in Figs. 10 and 11.

Table 7. Main formulae of prediction models

Model	Formulae
B4	$\varepsilon_{cs}(\tilde{t},\tilde{t}_c) = \varepsilon_{sh}(\tilde{t},\tilde{t}_c) + \varepsilon_{au}(\tilde{t},\tilde{t}_c)$ $\varepsilon_{sh}(\tilde{t},\tilde{t}_c) = \varepsilon_{shu}(\tilde{t}_c)\, k_h S(\tilde{t})$ $\varepsilon_{au}(\tilde{t},\tilde{t}_c) = \varepsilon_{au\infty}\left[1 + \left(\frac{\tau_{au}}{\tilde{t}+\tilde{t}_c}\right)^{\alpha}\right]^{r_t}$
fib MC2010	$\varepsilon_{cs}(t,t_c) = \varepsilon_{sh}(t,t_c) + \varepsilon_{au}(t)$ $\varepsilon_{sh}(t,t_c) = \varepsilon_{shu} k_{h,T} S(t-t_c)$ $\varepsilon_{au}(t) = \varepsilon_{au0}(f_{cm28}) \cdot \beta_{as}(t)$ $\varepsilon_{au0}(f_{cm28}) = -\alpha_{as}\left(\frac{0.1 \cdot f_{cm28,T}}{6 + 0.1 \cdot f_{cm28,T}}\right)^{2.5} \cdot 10^{-6}$ $\beta_{as}(t) = 1 - \exp\left(-0.2 \cdot \sqrt{t}\right)$

Model	Formulae
ACI 209R-92	$\varepsilon_{cs}(t,t_c) = \dfrac{(t-t_c)}{f+(t-t_c)} \cdot \varepsilon_{shu}$ $f = 26\exp\left[1.42\times10^{-2}(V/S\ )\right]$
JSCE-SCC (Aslani)	For normal strength ($f_{cm28} \le 55$ MPa): $\varepsilon_{cs}(t,t_c) = \left\{1-\exp\left[-0.1(t_T-t_{c,T})^{[-2.4(c/cm\ )+2.3]}\right]\right\}\cdot\varepsilon_{sh}$ For high strength ($55 < f_{cm28} \le 100$ MPa): $\varepsilon_{cs}(t,t_c) = \varepsilon_{sh}(t,t_c) + \varepsilon_{au}(t,t_c)$ $\varepsilon_{sh}(t,t_c) = \varepsilon_{shu}\dfrac{t_T-t_{c,T}}{\beta+(t_T-t_{c,T})}$ $\varepsilon_{au}(t) = \varepsilon_{au\infty}\left\{1-\exp\left[-a\cdot(t_T-t_c)^b\right]\right\}$
CEB90-SCC (Poppe)	$\varepsilon_{cs}(t,t_c) = \varepsilon_{cs0}S\ (t-t_c)$ $\varepsilon_{cs0} = \varepsilon_s(f_{cm28})\,k_h$ $\varepsilon_s(f_{cm28}) = \left[\dfrac{160}{1-\alpha_p\,(w/c\ )} + 10\beta_{sc}\,(9-0.1f_{cm28,T})\right]10^{-6}$ $k_h = -1.55\cdot\left[1-\left(\dfrac{RH}{100}\right)^3\right]$ $S\ (t-t_c) = \left(\dfrac{(t-t_c)}{(t-t_c)+45.5\cdot h_T^2}\right)^{\gamma}.$

Note: ε_{cs} is total shrinkage strain (10^{-6} m/m); ε_{sh} is drying shrinkage strain (10^{-6} m/m); ε_{au} is autogenous shrinkage strain (10^{-6} m/m); $\varepsilon_{au\infty}$ is final autogenous shrinkage strain (10^{-6} m/m); τ_{au} is autogenous shrinkage haftime; t is current age of the concrete (days); t_c is age at the end of moist curing (days); t_T, are temperature corrected exposure durations (days); $t_{c,T}$, are temperature corrected ages at exposure (days); RH is relative humidity (%); w is water (kg); c is cement (kg); cm is cementitious material (kg); f_{cm28} is mean 28-day compressive strength (MPa); $f_{cm28,T}$ is mean temperature adjusted 28-day compressive strength (MPa); V/S is volume-surface area ratio of specimen (mm); h_T is notional size (mm); k_h is humidity factor for shrinkage; $k_{h,T}$ is temperature corrected humidity factor; $S\,(t-t_c)$ is function defining the shape of shrinkage curve; β_{as} is time dependency of shrinkage; α_{as}, β_{sc} are coefficients depending the cement type; a, b are coefficients depending w/c ratio; α_p, γ are coefficients relating the cement to powder ratio.

4.1. Autogenous shrinkage

The prediction results of the models for autogenous shrinkage have yielded the findings presented in Fig. 10. As a result, the model B4TW-SCC predicted the highest efficiency in the compared models. The error of this model was about 52.3 % based on the *NRMSE* coefficient, which was the lowest value in comparison with the last prediction models as shown in Fig. 12. Moreover, the data points of the model B4TW-SCC were closely scattered around the standard line, which had predicted values equal to the test data, and most of the points fell within an acceptable range of ±40 %, as indicated by the two red dashed lines in the diagram. In contrast, predicted points of the model B4 were scattered broadly in the diagram with the *NRMSE* of 99.3 %. Besides, the model fib MC2010 predicted the lowest accuracy for autogenous shrinkage with the *NRMSE* approach of 104 %, and the model data points of this model tend closely towards the x-axis. Consequently, the inaccuracy of the models B4 and fib MC2010 is remarkably higher than that predicted by the newly developed prediction model.

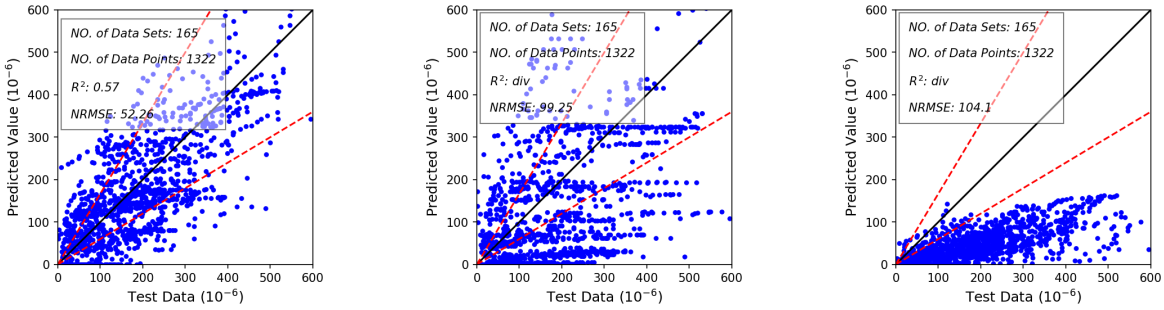

(a) B4TW-SCC (b) B4 (c) fib MC2010

Figure 10. Assessment of the prediction models for autogenous shrinkage

4.2. Total shrinkage

The model B4TW-SCC also accurately predicts the total shrinkage based on the SCC database, encompassing 843 datasets, as illustrated in Fig. 11. The investigation indicated that the model B4TW-SCC yields a minimum error, with the statistical indicators R^2 of 0.53 and *NRMSE* of 50.5 %. In contrast to the model B4TW-SCC, the original model B4 has a higher error with the *NRMSE* of 77 %. Besides, the other prediction models of conventional concrete have the *NRMSE* of 61 % for the model fib MC2010, and 64 % for the model ACI 209R-92. Moreover, most data points of the model JSCE-SCC (Aslani) tended towards the *y*-axis, allowing this model to overestimate the total shrinkage. Notably, the model CEB90-SCC (Poppe) had the maximum error, with an *NRMSE* value exceeding 360 %, as shown in Fig. 12.

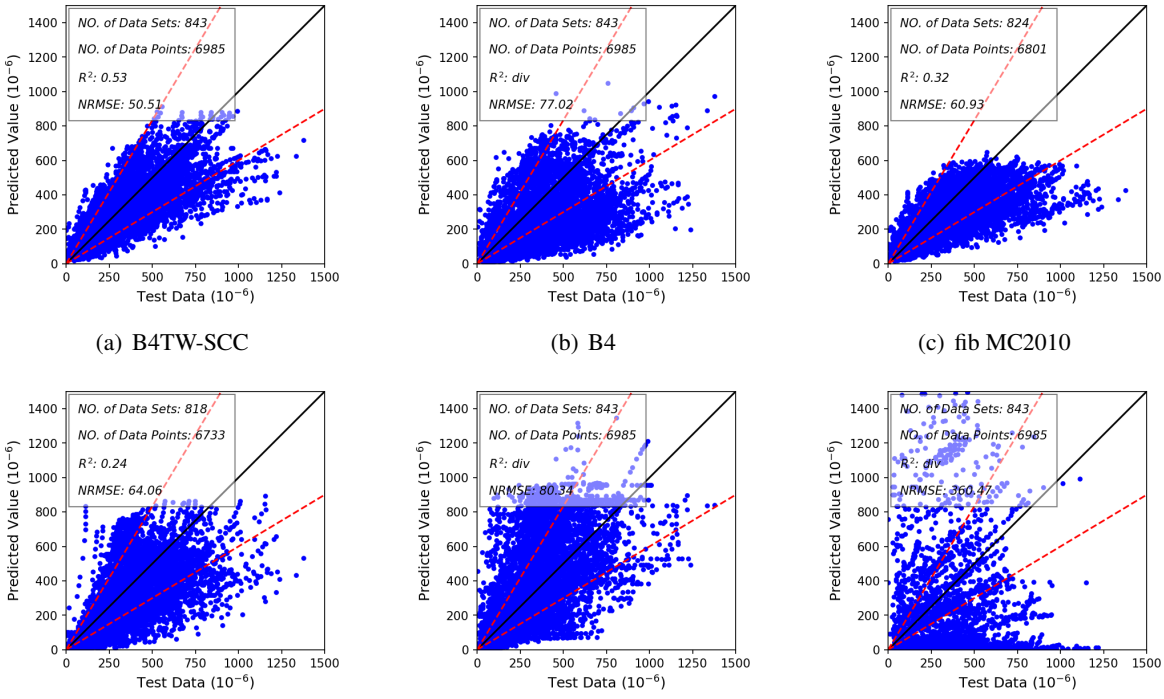

(a) B4TW-SCC (b) B4 (c) fib MC2010

(d) ACI 209R-92 (e) JSCE-SCC (Aslani) (f) CEB90-SCC (Poppe)

Figure 11. Assessment of the prediction models for total shrinkage

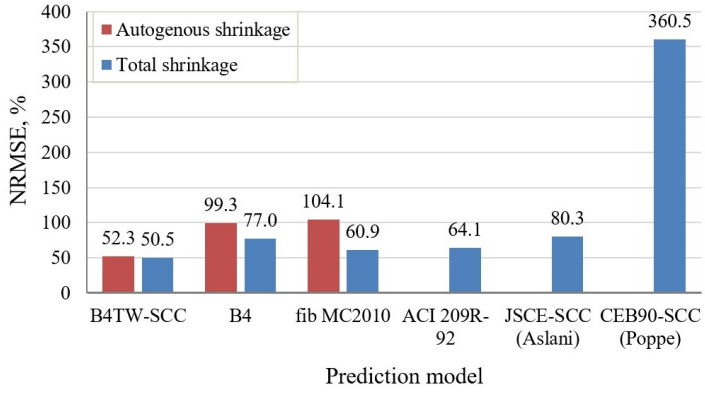

Figure 12. Evaluation of the models based on *NRMSE* values

5. Conclusion

According to the optimization of the model B4TW-SCC based on the combination of both statistical coefficients and the weighting scheme of the SCC database, the conclusions could be summarized as follows:

(1) The prediction formulae of model B4TW-SCC were calibrated using the new average composition of the SCC database , which comprises 1,316 curves for shrinkage.

(2) The new basic parameters of the model B4TW-SCC were optimized with 7 and 9 values for autogenous shrinkage and total shrinkage of SCC using pure cement, respectively.

(3) The novel scaling factors were introduced to predict the shrinkage of SCC containing powder and supplementary cementitious materials up to 36 values, compared to the original model B4.

(4) The model B4TW-SCC demonstrated the best prediction for the autogenous shrinkage strain and total shrinkage strain of SCC, compared to other available models.

The accuracy of parameter values was limited significantly by the range of the SCC database. The formulae of the modified model also cannot explicitly reflect the interaction between complicate factors and the shrinkage strain. Therefore, the shrinkage prediction of SCC could be improved by updating the laboratory database in further work. Additionally, the integration of shrinkage prediction with machine learning algorithms was also a potential research field.

References

[1] Mehta, P. K., Monteiro, P. J. M. (2006). *Concrete - Microstructure, properties, and materials*. New York: McGraw Hill.

[2] Abdalhmid, J. M., Ashour, A. F., Sheehan, T. (2019). Long-term drying shrinkage of self-compacting concrete: Experimental and analytical investigations. *Construction and Building Materials*, 202:825–837.

[3] Šahinagić-Isović, M., Markovski, G., ĐeĐeze, M. (2012). Shrinkage strain of concrete - causes and types. *Journal of the Croatian Association of Civil Engineers*, 64(9):727–734.

[4] Güneyisi, E., Gesoğlu, M., Özbay, E. (2010). Strength and drying shrinkage properties of self-compacting concretes incorporating multi-system blended mineral admixtures. *Construction and Building Materials*, 24(10):1878–1887.

[5] Leemann, A., Lura, P., Loser, R. (2011). Shrinkage and creep of SCC – The influence of paste volume and binder composition. *Construction and Building Materials*, 25(5):2283–2289.

[6] Rozière, E., Granger, S., Turcry, P., Loukili, A. (2007). Influence of paste volume on shrinkage cracking and fracture properties of self-compacting concrete. *Cement and Concrete Composites*, 29(8):626–636.

[7] ACI 237R-07 (2007). *Self-Consolidating Concrete*. Farmington Hills, MI: American Concrete Institute.

[8] Křístek, V., Šmerda, Z. (1988). *Creep and shrinkage of concrete elements and structures*. New York: Elsevier.
[9] ACI 209R-92 (1992). *Prediction of creep, shrinkage, and temperature effects in concrete structures*. Farmington Hills, MI: American Concrete Institute.
[10] CEB90 (1991). *CEB-FIP model code 1990 (MC90)*. Comité Euro-International du Béton, Geneva.
[11] fib 2010 (2013). *fib Model Code for Concrete Structures 2010*. Geneva.
[12] AASHTO (2017). *AASHTO LRFD bridge design specifications*. Washington, DC.
[13] Gardner, N. J., Lockman, M. J. (2001). Design provisions for drying shrinkage and creep of normal-strength concrete. *ACI Materials Journal*, 98(2):159–167.
[14] JSCE (2007). *Standard specifications for concrete structures 'Design'*. Tokyo.
[15] ACI 209.2R-08 (2008). *Guide for Modeling and Calculating Shrinkage and Creep in Hardened Concrete*. Farmington Hills, MI: American Concrete Institute.
[16] Baweja, S., Bažant, Z. P. (1995). Creep and shrinkage prediction model for analysis and design of concrete structures - model B3. *Materials and Structures*, 28(6):357–365.
[17] Bažant, Z. P., Wan-Wendner, R. (2015). Model B4 for creep, drying shrinkage and autogenous shrinkage of normal and high-strength concretes with multi-decade applicability. *Materials and Structures*, 48(4): 753–770.
[18] Huang, H.-C. (2020). Regression of Shrinkage and Creep Prediction Formula of Concrete in Taiwan Based on Database Analysis and Application on Long-term Deflection of Prestressed Concrete Bridge. Master's thesis, National Taiwan University, Taipei, Taiwan (ROC). In Chinese.
[19] Poppe, A.-M., De Schutter, G. (2005). Creep and shrinkage of self-compacting concrete. In *First International Symposium on Design, Performance and Use of Self-Consolidating Concrete*, Champs-sur-Marne, France.
[20] Aslani, F., Maia, L. (2013). Creep and shrinkage of high-strength self-compacting concrete: Experimental and analytical analysis. *Magazine of Concrete Research*, 65(17):1044–1058.
[21] Bažant, Z. P. (1988). *Mathematical modelling of creep and shrinkage of concrete*. New York: John Wiley & Sons.
[22] Hubler, M. H., Wendner, R., Bažant, Z. P. (2015). Comprehensive Database for Concrete Creep and Shrinkage: Analysis and Recommendations for Testing and Recording. *ACI Materials Journal*, 112(4): 547–558.
[23] Kwon, S. H., Zi, G., Kim, N. Y. (2013). KCI Database of Test Data for Creep and Shrinkage of Concrete. In *Advances in Structural Engineering and Mechanics*, Jeju, Korea.
[24] Sakata, K., Ayano, T., Imamoto, K., Sato, Y. (2008). Database of creep and shrinkage based on Japanese researches. In *CONCREEP 8*, Ise-Shima, Japan.
[25] Montgomery, D. C., Peck, E. A., Vining, G. G. (2012). *Introduction to Linear Regression Analysis*. New Jersey: John Wiley & Sons.
[26] Hami, A. E., Pougnet, P. (2020). *Embedded Mechatronic Systems 2 - Analyses of Failures, Modeling, Simulation and Optimization*. New York: Elsevier.
[27] Dietterich, H. R., Lev, E., Chen, J., Richardson, J. A., Cashman, K. V. (2017). Benchmarking computational fluid dynamics models of lava flow simulation for hazard assessment, forecasting, and risk management. *Journal of Applied Volcanology*, 6(9):1–14.
[28] Rizi, F. S., Granitzer, M. (2017). Properties of Vector Embeddings in Social Networks. *Algorithms*, 10 (109):10040109.
[29] Wendner, R., Hubler, M. H., Bažant, Z. P. (2015). Optimization method, choice of form and uncertainty quantification of Model B4 using laboratory and multi-decade bridge databases. *Materials and Structures*, 48:771–796.
[30] Hubler, M. H., Wedner, R., Bažant, Z. P. (2015). Statistical justification of Model B4 for drying and autogenous shrinkage of concrete and comparisons to other models. *Materials and Structures*, 48:797–814.
[31] Bažant, Z. P., Li, G.-H. (2007). Unbiased Statistical Comparison of Creep and Shrinkage Prediction Models. Technical report, Evanston, Illinois.

[32] Chan, Y. W., Liu, C. Y., Lu, Y. S. (1998). Effects of slag and fly ash on the autogenous shrinkage of high performance concrete. In *Proceedings of the International Workshop organized by JCI*, Hiroshima, Japan.

[33] Kristiawan, S. A., Aditya, M. T. M. (2015). Effect of high volume fly ash on shrinkage of self-compacting concrete. *Procedia Engineering*, 125:705–712.

[34] Şahmaran, M., Lachemi, M., Erdem, T. K., Yücel, H. E. (2011). Use of spent foundry sand and fly ash for the development of green self-consolidating concrete. *Materials and Structures*, 44:1193–1204.

[35] Zhao, H., Sun, W., Wu, X., Gao, B. (2015). The properties of the self-compacting concrete with fly ash and ground granulated blast furnace slag mineral admixtures. *Journal of Cleaner Production*, 95:66–74.

[36] Jun, C., Gengying, L. (2016). Mechanical properties and drying shrinkage of self-compacting concrete containing fly ash. *Romanian Journal of Materials*, 46(4):480–484.

[37] Niknezhad, D., Kamali-Bernard, S., Garand, C. (2015). Influence of mineral admixtures (Metakaolin, slag, fly ash) on the plastic, free, and restrained shrinkage of SCCs. In *CONCREEP 10*, Vienna, Austria.

[38] Yasumoto, A., Edamatsu, Y., Mizukoshi, M., Nagaoka, S. (1998). A study on the shrinkage crack resistance of self-compacting concrete. In *Symposium Paper*, volume 179, 651–670.

[39] Wang, H.-Y., Lin, C.-C. (2013). A study of fresh and engineering properties of self-compacting high slag concrete (SCHSC). *Construction and Building Materials*, 42:132–136.